HiSST: 3rd International Conference on
High-Speed Vehicle Science Technology
14 -19 April 2024, Busan, Korea

Thermally choked nozzle flow 1D model for low-Mach dual mode scramjet performance assessment

J.E. Durand[1] and F. Olivon[2]
DMPE, ONERA, Université Paris-Saclay F-91123 Palaiseau- France

Abstract

Beyond the flight Mach number 7, the scramjet, with supersonic combustion, shows higher performances than the ramjet, with subsonic combustion, due to the substantial pressure losses, chemical dissociation effects, and high thermomechanical stresses. The dual-mode scramjet would be a solution to hold optimal performances over an extensive range of flight Mach numbers. The use of a divergent nozzle choked flow through a thermal throat, generated by heat combustion, turns out to be an elegant approach to switch from subsonic to supersonic combustion processes, avoiding mechanical constraints and complex systems. Furthermore, compared with conventional ramjet, this approach increases the allowable mass flow rate through the engine, increasing the thrust. However, to design such a combustion chamber configuration, the flow and performances require to be modeled according to the characteristics of the combustion, the turbulence, and the significant variations of the thermos-physical properties. The present work aims to develop a quasi-one-dimensional steady model of a thermally choked nozzle flow (TCNF) to improve the quasi-one-dimensional model of a dual-mode scramjet and to predict the performances. Three approaches are assessed according to assumptions on thermos-physical properties, the friction effects, and the aerothermal flow. Numerical simulations, computed with CEDRE, the ONERA CFD software, will be carried out to validate the obtained results in the quasi-one-dimensional model. The impact of mass flow rate and equivalence ratio is studied. The turbulent boundary layer impact, via friction, on the thermal throat position is also regarded.

Keywords: *Thermal throat, Dual-mode scramjet, Aerothermal flow, turbulence, Performance assessment*

Nomenclature

A – Cross Section area (m^2)
Cp – Heat capacity (J/kg/K)
Cf – Friction coefficient
D_h – Hydraulic diameter (m)
h – Divergent nozzle height (m)
H – Enthalpy (J/kg)
L – Divergent nozzle length (m)
M – Mach number
$\dot{m}$ – Mass flow rate (kg/s)
q – Energy added to the flow (kJ/kg)
r – Specific gas constant (J/kg/K)
R – Reduced mass flow rate
T – Temperature (K)
W – Molar mass (kg/mol)
$\dot{W}_T$ – Reaction rate (W/m^3)
x – Axial coordinate (m)

Greek
γ – Adiabatic coefficient
ϕ – Equivalence ratio
ω – Scalar turbulent dissipation (s^{-1})

Subscripts
e – exterior (core flow)
i – inlet
t – stagnation condition
tht – thermal throat condition

[1]Research Engineer, Energetics Department, jean-etienne.durand@onera.fr
[2]Ph.D. student, Energetics Department, frederic.olivon@onera.fr

Copyright © 2024 by author(s)

1. Introduction

The dual-mode ramjet configuration using a divergent thermally choked nozzle flow turns out to be an elegant approach to switch from subsonic to supersonic combustion processes, avoiding mechanical constraints and complex systems. Compared with conventional ramjet, this approach increases the allowable mass flow rate through the engine, increasing the thrust. However, the dual-mode ramjet design requires an efficient quasi-one-dimensional combustion chamber model to assess the performances because of the strong flow dependence on the heat release distribution. Numerous quasi-one-dimensional models have been developed, particularly in the last decades [1-4]. O'Brian *et al.* [5] have given the basis of the finite rate chemistry-based model coupled with the quasi-one-dimensional inviscid model of Shapiro [6]. The focus on finite rate chemistry comes from the fact that complex chemistry can also have a direct effect on thrust [1]. In contrast, Birzen & Doolan [7] have proposed a quasi-one-dimensional model with combustion based on mixing-limited rather than chemistry combustion models. According to the authors, this approach is justified when the model is compared with experimental results. Torrez *et al.* [1], developed a quasi-one-dimensional model, derived from O'Brien ODEs, to investigate the shock and dissociation effects in scramjet engines. The investigators included precombustion shock, fuel mixing, and finite rate chemistry models. The model can solve for both subsonic and supersonic flows [8]. Ispir *et al.* [9], to develop a robust DMR model for nose-to-tail simulations, uses the same formulation. Torrez *et al.* [2,3,4] then improved the model by considering finite-rate chemistry via the Stationary Laminar Flamelet Model (SLFM). This approach uses a flamelet solution based on an assumed PDF model for each parameter. The probability distribution function (PDF) approach includes the effects of different strain fields, species and momentum diffusions, and turbulence, as the duct velocity and fuel jet velocity change. The PDF-based chemistry is tabulated [8]. To avoid difficulties in solving the sound speed, the problem is formulated according to velocity instead of the Mach number approach, giving an easier set of equations [10]. This model has been integrated into a scramjet engine model called MASIV [2], developed by the University of Michigan, to predict the thermal throat position and the performances [10].

Zhang *et al.* [11] have developed a quasi-one-dimensional model by coupling the equations of O'Brien *et al.* [5] with a regenerative cooling model to study the heat transfer behavior through the cooled scramjet chamber wall. Çakir *et al.* [12], to assess the performance of intakes for high-speed propulsion systems, use the formulation of Zhang *et al.* [11] even though the cooling model is not considered. For TBCC application, Connolly *et al.* [13] have developed a one-dimensional model in NPSS based on the approach of Smart [14], using a rearranged form of Shapiro's isentropic equations, approximations of the mixing and the combustion heat release of Heiser & Pratt [15], and a simple wall heat flux model. Owing to the structure of NPSS, the model can interface with a cooling system. To rebuild some quantity features of the flow from experimental measurements, Li *et al.* [16] developed a 1D analysis method based on the classical ODEs for diabatic flow through variable cross sections, rearranged to deduce the Mach number and stagnation temperature from pressure measurements and the geometry. The friction coefficient is however set. Seleznev *et al.* [17] have proposed to compare a quasi-one-dimensional, derived from O'Brien *et al.* [5] and Birzer *et al.* [7] approaches, and a two-dimensional model to highlight the element of the flow field structure not predicted by the quasi-1D model. Tian *et al.* [18] developed a quasi-one-dimensional method with a new model for precombustion shock trains for simulating the different modes in the dual-mode scramjet flowfield. The release of energy is obtained from a fuel-mixing model or an imposed heat release distribution estimated from experimental results. However, no explicit formulation of species mass fraction is given. According to Torrez et al. [10], the derivatives of gas properties are small compared with the Mach number space derivative. Hence, the effects of variations of thermos-physical properties are not taken into account. However, no quantitative evidence has been shown or reported.

In the present study, a quasi-one-steady steady model for a thermally choked nozzle flow (TCNF) is developed to predict the potential performances of a low-Mach dual-mode scramjet engine and to distinguish the associated contribution of considered physical phenomena involved in a TCNF. An auxiliary function is introduced to avoid the singularity at M =1 to solve the Mach number-based equation of Shapiro [6] with first-order schemes. Several approaches are assessed according to assumptions on thermos-physical properties, the friction effects, and the aerothermal flow. The objective is to measure the improvement of the performances and flow features compared with a more complex approach and to find an efficient compromise. Numerical simulations, computed with CEDRE, the ONERA CFD software, will be carried out to validate the obtained results with the quasi-one-

Copyright © 2024 by author(s)

dimensional model. The impact of mass flow rate and equivalence ratio is studied. First, the methodology is explained and the case of the study is presented. The models and their methods and assumptions are exposed. Then, the models are compared with each other and the numerical simulations.

2. Methodology

A quasi-one-dimensional steady model of a thermally choked nozzle flow is proposed. To catch the contribution of the temperature and species variations of thermos-physical properties of the fluid and the effects of friction on the TCNF, a validation process must be carried out by comparing the results of the quasi-one-dimensional model with a more realistic approach, such as CFD simulations. For simplicity, only 2D simulations are considered. Because of the complexity of a real turbulent flame in terms of modeling, in this study, the quasi-one-dimensional model uses directly the heat release profile obtained in the CFD simulations. Future studies will consider combustion modeling to improve the current approach.

The reference case considers the conditions described in Table 1, representative of the conditions found in a low-Mach dual-mode scramjet, before the combustion process. With these conditions, the Mach number at the inlet varies but covers the highly compressible subsonic regime.

Table 1: Reference case.

$\dot{m}_{in}$ (kg/s)	Tt (K)	ϕ
10	600.7	1.0

The equivalence ratio and the mass flow rate are the design parameters used to validate the quasi-1D models. The associated ranges are respectively 0.6, 0.8, 1, 1.2, and 5, 10, 20, 30 kg/s.

Three models based on the equations derived by Shapiro [6] are compared:

- Model M1: Mach number evaluation with constant adiabatic coefficient and heat capacity. This model needs to set the values of these two thermos-physical properties. In this study, the initial and critical conditions are used to assess the improvement by resetting these properties;
- Model M2: Mach number evaluation with temperature dependence of heat capacity and a fixed composition. The purpose is to assess the improvement of considering temperature dependence on the performance prediction. In this study, two formulations of the same equation of Shapiro have been considered and compared with each other for the thermal position detection and resolution;
- Model M3: Mach number evaluation with dependence on temperature and species composition of heat capacity and adiabatic coefficient. The proposed model in this model is not complete because the purpose is only to observe the deviation of performances when considering the variations of thermos-physical properties with the composition of the fluid.

The effect of friction is also considered to assess its effects on defining the TCNF. Then, a model based on these observations is proposed.

3. Numerical simulation model

3.1. Numerical reference case

To validate the quasi-one-dimensional model for thermally choked flow in a divergent nozzle, 2D dimensional CFD calculations are carried out with the ONERA's multiphysics platform, CEDRE. The geometry is a divergent duct with an angle of aperture equal to 1.5° (Fig. 1). The 2D-dimensional flow evolves in an x-y plane with an invariance according to the z-axis. The inlet height is 70 mm and the length is 1 m. The calculations are performed only in half of the geometry due to the nozzle's plane of symmetry.

To generate the most uniform possible heat release, premixed combustion is considered. Hence, a premixed flow corresponding to a given equivalence ratio is injected into the nozzle inlet. To hold the

Copyright © 2024 by author(s)

flame, six flame-holder bases, regularly placed very close to the inlet, are designed with a thickness of 5 mm each. This injection system enables fostering a more uniform heat release, ensuring the comparison with quasi-one-dimensional model calculations. However, even though the heat release is conveniently set, the flow features a complex configuration with recirculation regions until 50 mm from the inlet.

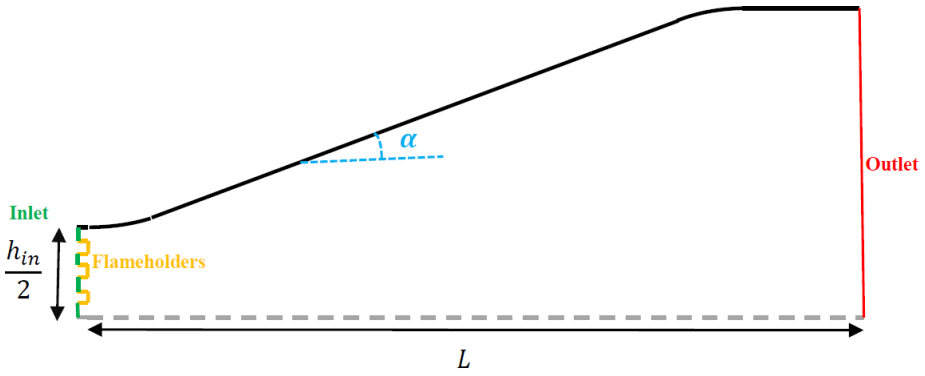

Figure 1: Geometry of the divergent duct.

In 3D configuration, the injection system is much less cumbersome than in 2D configuration where depth invariance does not allow more convenient geometry. Future studies will consider 3D configurations to attenuate the effects of the injection system on the velocity fields.

3.2. Numerical models and mesh

The mesh is structured with 500000 cells obtained by mesh convergence. The wake regions and the boundary layer regions are refined to catch the turbulence effects (Fig. 2).

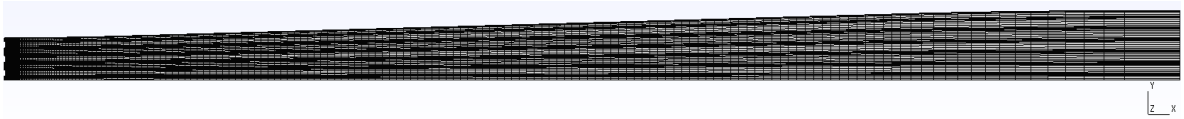

Figure 2: 2D structured mesh of the divergent duct.

The flow is multi-species in the gaseous phase. The spatial integration is performed with 2nd order centered schemes. As only steady solutions are considered, the temporal integration is realized with an implicit 1st order scheme with the local time steps. The convergence of local time steps is checked after convergence. The reference time step is equal to 5.10^{-7} s.

The turbulence is simulated with the RANS k-w SST approach. The minimal cell size is $1.9\ 10^{-6}$ m to reach the condition y+ = 1. At the inlet, the turbulence intensity is set at 5 %, typical for intern flows, and the characteristic length is chosen equal to 10% of the initial height. The heat release is obtained by the premixed combustion of Decane with the air. The combustion is modeled with the "Relaxation to Equilibrium" model, which considers the local thermochemical equilibrium in the flow to compute the species production rates. This model depends also on a constant set to 1 and the turbulent frequency is written as:

$$f_t = C_\mu \omega \quad with\ C_\mu = 0.09 \qquad (1)$$

6 species are considered: C10H22, O2, N2, CO, CO2 and H2O. The choice of this model is due to simplicity to obtain reasonable results with the effects of turbulence on the flame.

The flow is first computed in frozen conditions before activating the combustion model. During this first step, the static pressure is imposed at the outlet. When the flow reaches substantially the supersonic regime, a supersonic outlet is then applied. At the inlet, the mass flux is imposed with the stagnation temperature. Hence, the inlet pressure and Mach number values vary according to the simulated case.

Copyright © 2024 by author(s)

4. Quasi-1D models

4.1. Quasi 1D equations and thermal throat definition

The model for the core flow is based on the Mach number equation established by Shapiro [1] from the generalized one-dimensional flow equations by considering the effects of divergent duct, the heat addition due to combustion and the friction of flow on the duct wall.

$$\frac{1}{M}\frac{dM}{dx} = -\frac{\left(1+\frac{\gamma-1}{2}M^2\right)}{1-M^2}\left(\frac{1}{A}\frac{dA}{dx} - \frac{2\gamma M^2 C_f}{D_h} - \frac{\left(1+\gamma M^2\right)}{2\left(1+\frac{\gamma-1}{2}M^2\right)}\left(\frac{1}{CpT}\frac{dq}{dx} - \frac{1}{W}\frac{dW}{dx}\right)\right) - \frac{1}{2\gamma}\frac{d\gamma}{dx} \quad (2)$$

The hydraulic diameter D_h is obtained as twice of the height of the cross section, considering the wetted surface located only the upper and the lower surfaces as plane geometry is assumed with a z-axis invariance. The friction coefficient is determined by using the correlation of De Chant *et al.* [19], developed for compressible flow, assuming smooth walls ($k^+ = 0$).

As observed by Shapiro [6], Eq. 2 shows a singularity when the flow reaches the sonic speed. Zierep [20] noted that, in the case of Euler flows (Cf = 0) with a constant adiabatic coefficient, Eq. 3 must be verified when M = 1, to avoid unphysical solution:

$$\frac{1}{A}\frac{dA}{dx} = \frac{1}{C_pT}\frac{dq}{dx} \; at \; M = 1 \quad (3)$$

When the flow is initially subsonic, the heat addition must be large enough compared to the divergent duct aperture to increase the Mach number until reaching M = 1 where the heat decrease meets the effects of the divergent duct. Then, the effects of heat addition, become marginal compared with the duct aperture, and the Mach number goes on increasing because of the supersonic flow in a divergent duct. This sonic point, ensuring a continuous solution of Eq. 2 is called thermal throat.

To solve Eq. 2, Shapiro [1] has proposed a method to determine the Mach number gradient at the critical point by using the l'Hôpital rule. Heiser & Pratt [15] have designed an approach consisting of identifying the singularity with the use of L'hôpital's rule, then integrating backward from the calculated thermal throat position to the inlet. Torrez et al. [10] replaced this approach with a shooting method, attempting to concur with the inlet Mach number to avoid physical inconsistencies of ODEs at M = 1, where the singularity appears. This method is particularly suited when the heat released by the combustion is not specified initially. Contrary to O'Brien-based approaches using the velocity approach, the Mach number-based models require, to ensure stability, the use of a second-order Runge Kutta formulation, near singularities such as the sonic point [13].

In the present study, a similar method of Heiser & Pratt [15] is used. Eq. 2 is reformulated by introducing an auxiliary function to avoid the singularity term. This approach eases the resolution of the problem with a simple 1st order Euler method. According to assumptions made on the properties of the flow, the auxiliary function would be different, adapted to the treated case.

4.2. Model with constant adiabatic coefficient

In the case of a constant adiabatic coefficient, Eq. 2 can be rewritten as:

$$\frac{d\phi(M)}{dx} = \frac{1}{A}\frac{dA}{dx} - \frac{2\gamma M^2 C_f}{D_h} - \frac{\left(1+\gamma M^2\right)}{2CpT\left(1+\frac{\gamma-1}{2}M^2\right)}\frac{dq}{dx} \quad (4)$$

with

$$\phi(\mathrm{M}) = \ln\left(\frac{1}{\mathrm{M}}\left[\frac{2}{\gamma+1}\left(1+\frac{\gamma-1}{2}\mathrm{M}^2\right)\right]^{\frac{\gamma+1}{2(\gamma-1)}}\right) \quad (5)$$

Copyright © 2024 by author(s)

The auxiliary function, in this case, has a physical meaning, describing a logarithmic variation of the reduced mass flow compared with the critical state:

$$\phi(\mathrm{M}) = -ln\left(\frac{R(M)}{R_{th}}\right), with\ R(M) = \frac{\dot{m}\sqrt{T_t}}{P_t A} = \sqrt{\frac{\gamma}{r}}\frac{M}{\left(1+\frac{\gamma-1}{2}\mathrm{M}^2\right)^{\frac{\gamma+1}{2(\gamma-1)}}} \quad (6)$$

In a particular case, assuming an isentropic flow, the classical formula describing the evolution of Mach number in a convergent/divergent duct with a choked geometrical throat is naturally obtained [6].

4.3. Resolution methodology

Eq. 4 shows no singularity. Furthermore, the auxiliary function displays a minimal value equal to zero at M = 1. Besides, Eq. 4 turns out to possess a minimal value as well in the case of the thermal throat formation. Hence, the necessary and sufficient condition to reach the thermal throat is:

$$if\ \frac{dq}{dx}(x_{tht}) \neq 0\ and\ M_{inlet} < 1, \qquad thermal\ throat\ at\ x_{tht} \Leftrightarrow \begin{cases} \frac{d\phi}{dx}(x_{tht}) = 0 \\ \phi(x_{tht}) = 0 \end{cases} \quad (7)$$

In the present study, the reaction rate obtained by CFD computation is transformed on a so-called heat addition for the quasi-one-dimensional models. Hence, to solve Eq. 3, the thermal throat position is firstly determined with the knowledge of the heat amount added to the flow and the geometry variations. Depending on the critical state, only the properties implied in the terms of the equation at the thermal throat can be obtained by assuming the constant adiabatic coefficient and heat capacity of the flow.

After determining the thermal throat position, the subsonic part of the Mach number variations are backwardly calculated from the thermal throat to the inlet with Eq. 3. Then, with the same approach, but forwardly, the Mach number of the supersonic part is also determined. At each iteration, the next step value of the auxiliary function is obtained from Eq. 4. With an inverse method and assuming the calculation location in the subsonic or the supersonic region of the flow, the Mach number is obtained. The static temperature, on which depends the terms of Eq. 4, is obtained from the stagnation temperature, which is altogether determined by the heat addition function imposed in the calculation:

$$T_t(x) = T_{t,i} + \frac{q(x)}{C_p}\ and\ T(x) = \frac{T_t(x)}{\left(1+\frac{M(x)^2\gamma r T(x)}{C_p}\right)} \quad (8)$$

Hence, the Mach number and static temperature fields are completely determined. The other quantities are obtained from a given value of mass flow rate. This process was already employed by Olivon *et al.* [21].

4.4. Model with temperature dependent adiabatic coefficient

When the adiabatic coefficient of the flow varies with the temperature, the auxiliary function (Eq. 5) cannot be used. Another function with similar properties is therefore proposed, based only on the Mach number:

$$\theta(\mathrm{M}) = \frac{1-M^2}{2} + ln(M) \quad (9)$$

The equation to solve is thereby written as:

$$\frac{d\theta(M)}{dx} = -\left(1+\frac{\gamma-1}{2}M^2\right)\left(\frac{1}{A}\frac{dA}{dx} - \frac{2\gamma M^2 C_f}{D_h}\right) + \frac{(1+\gamma M^2)}{2}\left(\frac{1}{CpT}\frac{dq}{dx} - \frac{1}{W}\frac{dW}{dx}\right) + \frac{(M^2-1)}{2\gamma}\frac{d\gamma}{dx} \quad (10)$$

In the present case, the same resolution method can be used to solve Eq. 10. However, instead of considering a minimal value, a maximal value is reached at M = 1. The auxiliary function image is in the negative part of real numbers. At each step, a value of Mach number is obtained from the auxiliary function and the knowledge of the location of the flow regime. However, contrary to the last method,

Copyright © 2024 by author(s)

the variations of the adiabatic coefficient are required to be assessed. With temperature dependence only, the variations are directly associated with the variations of temperature:

$$\frac{1}{\gamma}\frac{d\gamma}{dx} = -(\gamma(\mathrm{T})-1)TK_T(T)\left(\frac{1}{T}\frac{dT}{dx}\right) \quad with\ K_T(T) = \frac{1}{C_p(T)}\frac{dC_p}{dT}(T) \tag{11}$$

Shapiro also has derived an equation describing the temperature variations which can be injected in Eq. 10:

$$\frac{d\theta(M)}{dx} = -\left(1+\frac{\gamma(\mathrm{T})-1}{2}M^2\left(1-(\gamma(\mathrm{T})-1)TK_T(T)\right)\right)\left(\frac{1}{A}\frac{dA}{dx}-\frac{2\gamma(\mathrm{T})M^2C_f}{D_h}\right) + \frac{\left(1+\gamma(\mathrm{T})M^2+(\gamma(\mathrm{T})-1)TK_T(T)\left(1-\gamma(\mathrm{T})\,M^2\right)\right)}{2Cp(T)T}\frac{dq}{dx} \tag{12}$$

Hence, Eq. 11 is therefore used to obtain the Mach number variations. Instead of using the stagnation temperature, total enthalpy formulation is used to determine the static temperature with a fixed point method:

$$H_t(x) = H_{t,i} + q(x) \ \ and\ T(x) \leftarrow H_t(x) = H(T) + \frac{M(x)^2\gamma(T)rT}{2} \tag{13}$$

The mass fraction species is also taken into account in the calculation of static temperature since the enthalpy depends on this distribution. Nevertheless, this method is applied with constant or variated species distribution.

5. Discussion results

5.1. Heat release model from the numerical results

From CFD calculations, the heat addition gradient is deduced from the heat released by the combustion of Decane/Air. Considering an elementary control volume of a steady flow between x and x+Δx, the heat addition gradient can be written as:

$$\forall x \in [0,L],\ \frac{dq}{dx}(\mathrm{x}) = \frac{\hat{q}_{x+\Delta x}-\hat{q}_x}{\Delta x} = \frac{1}{\dot{m}}\int_{-\frac{h(x)}{2}}^{\frac{h(x)}{2}}\dot{W}_T(x,y)dy \tag{14}$$

where $\hat{q}_x\ and\ \hat{q}_{x+\Delta x}$ is the mass flow rate weighted average of the heat addition through the cross section, respectively at x and x+dx. Thus, the heat addition gradient profiles for each equivalence ratio value are shown in the Fig. 3.

In contrast, the heat addition profiles are practically unchanged with the increase of the inlet mass flow rate at $\phi = 1$. This invariance is related to the combustion model depending on the turbulent frequency and the density of the flow. The turbulent frequency is approximately proportional to the square root of the turbulent kinetic energy which can be seen as proportional to the mean flow velocity. Hence, the reaction rate becomes proportional to the mass flux of the flow. The heat addition gradient becomes therefore little affected by the mass flow rate. These profiles are then imposed in the quasi-one-dimensional models to restitute the Mach number profiles.

Copyright © 2024 by author(s)

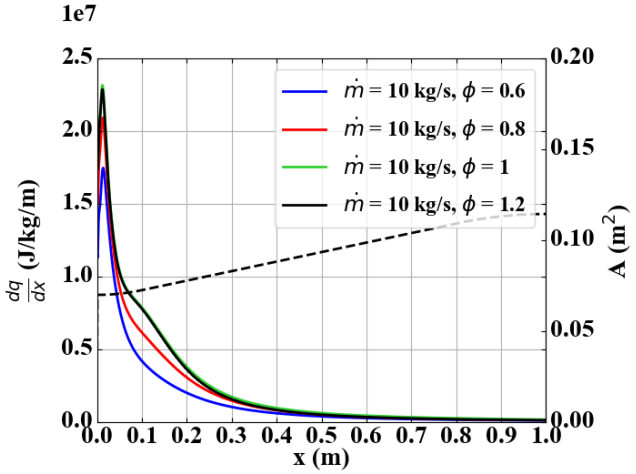

Figure 3: Heat addition profile along the divergent duct based on the reaction rate of 2D CFD flow calculation.

5.2. Quasi-one-dimensional models and CFD results comparison

Fig. 4 shows the Mach number profiles calculated by the quasi-one-dimensional model and the CFD simulations for 10 kg/s and $\phi = 0.6$. The trends are in good agreement with the simulation, even though model M1 underestimates the CFD data, whereas the model M2 overestimates it. Furthermore, the Mach number profiles seem shifted from the calculated values of the thermal throat position. Considering the comparison of model M2 with the CFD simulations, a backward difference of 1.6 % for the thermal throat position is directly correlated to the increase of 0.7 % for outlet Mach number.

Besides, in the flame-holder zone, the Mach number variations are much more erroneous due to the recirculation zones where only an empirical model is employed to attempt to correct the slowing down effect from the reduced cross-section area to the large cross section area in the subsonic regime.

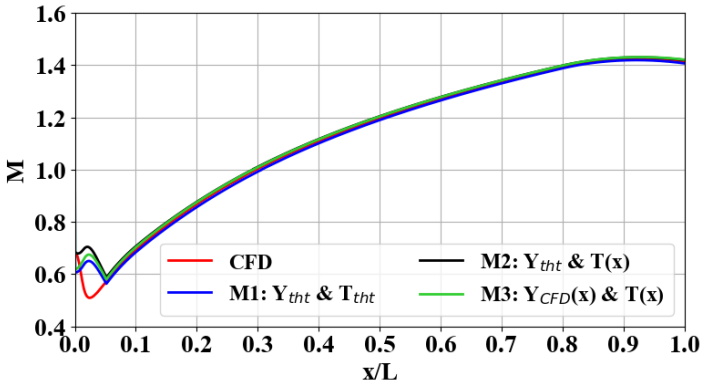

Figure 4: Mach number profile comparison between models and CFD for 10 kg/s and $\phi = 0.6$.

The net thrust is underestimated by all quasi-one-dimensional models. Nevertheless, model M3 shows the closest predictions (~ 1 %) due to the consideration of the effects of species distribution and temperature on the thermos-physical properties (Fig. 5). Nevertheless, model M2 based on the CFD species distribution at the thermal throat displays similar differences whereas an underestimation of 4-8 % is observed when using the inlet species distribution. For model M1, the thrust is underestimated by about 7 to 10 % when using the inlet species. However, this difference is reduced to 4-6 % with the thermal throat composition. Hence, using the local species distribution at the thermal throat improves significantly the prediction of the net thrust.

The maximum net thrust is reached when the mixture is stoichiometric. This condition matches with the farthest position of the thermal throat from the inlet. The coefficient α shows that almost 82 % of the net thrust is generated in the subsonic zone for CFD calculations and seems almost independent of

Copyright © 2024 by author(s)

the equivalence ratio. Nevertheless, a slight decrease is observed at lean conditions, showing insufficient energy released to hold the contribution of the subsonic part of the flow. When the mixture is leaner, the decrease of energy released in the flow is sharper and less extended (Fig. 3), changing therefore the thermal throat position closer to the inlet.

For the outlet pressure, all models display very close values between each other (Fig. 6). Nevertheless, the maximal underestimation is obtained with the model M2 using inlet species composition, estimated about 3 to 5 %. On another hand, for all models, the outlet Mach number differences are below 2 %, following the inverse trend as the thermal throat position. However, outlet static temperature displays discrepancies about 4-8 % for model M1, displaying the most underestimated net thrust values with model M2 using inlet species composition. For model M3, the calculated net thrust shows a good agreement with CFD simulations, explained by the fact that the outlet conditions are well reproduced. For the other cases, the impact of the outlet static pressure and temperature turn out significant, displaying underestimated net thrust.

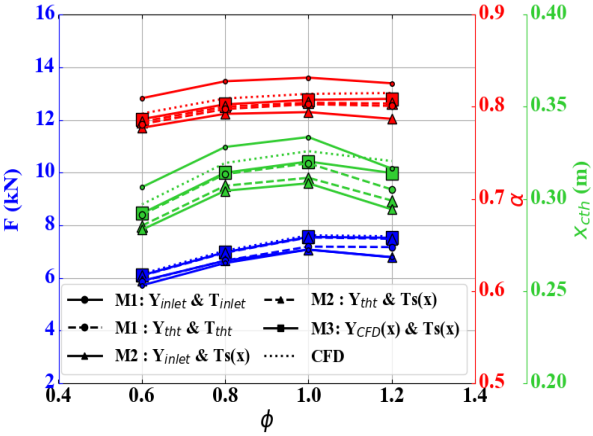

Figure 5: Net Thrust comparison between quasi-1D models and CFD, correlated with the thermal throat position, evolving with the equivalence ratio.

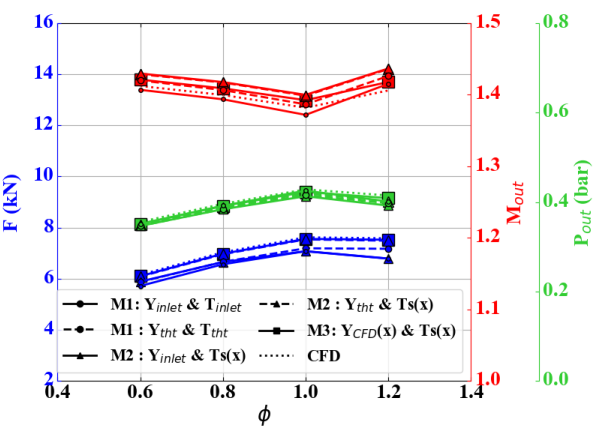

Figure 6: Outlet pressure and Mach number variations, evolving with the equivalence ratio.

Fig. 6 shows an increase in net thrust whereas the outlet Mach number decreases when the lean mixture is closer to the stoichiometry. Two parameters lead to the net thrust of a TCNF: the outlet temperature and pressure. When enriching the lean mixture with fuel, the critical temperature at the thermal throat increases until reaching a maximal value at the stoichiometric point (Fig. 7). The reason is the direct relation between the critical temperature and the heat released in the subsonic part of the flow, due to the choking flow conditions at the thermal throat.

Assuming a constant mass flow rate, the critical pressure and the cross-section area must increase to keep the critical conditions. In a divergent duct, the thermal throat goes therefore downstream and the critical pressure increases slightly, until reaching maximal values when the stoichiometric mixture is obtained. The downstream displacement of the thermal throat position reduces the distance between the sonic line (thermal throat) and the outlet. According to the observation of the Mach number profiles, the flow reaches a lower Mach number at the outlet. Nevertheless, this decrease is compensated by the increase in pressure and temperature at the outlet, as observed in Fig. 6.

Copyright © 2024 by author(s)

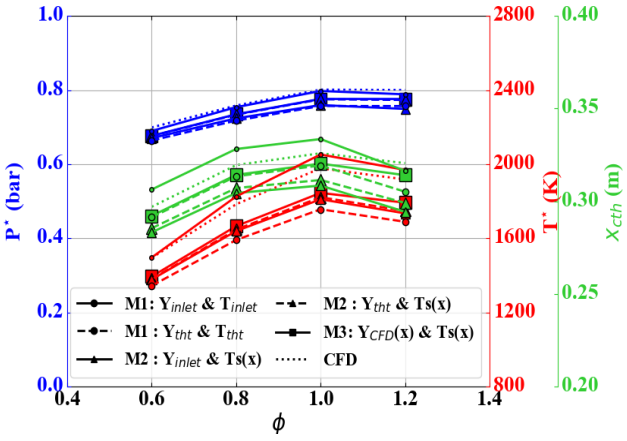

Figure 7: Variations of the critical conditions when increasing the equivalence ratio

In contrast, the increase in mass flow rate at the inlet does not affect, apparently, the thermal throat position and thrust distribution coefficient α (Fig. 8). The main reason is due to the insensitiveness of the heat addition gradient to the mass flow rate. The reaction rate displays a proportional behavior with the mass flow rate, leading to compensate for the mass flow rate dependence of advection terms to transport heat addition. Nevertheless, as expected, the net thrust increases proportionally with the mass flow rate. With a more realistic combustion model, such that uncoupling phenomena may not happen. A more detailed study is therefore needed to improve the trends related to the mass flow rate.

As for the analysis of the effect of the equivalence ratio on performance, model M3 shows the best prediction of net thrust (Fig. 8 & Fig. 9), whereas the outlet pressure given by all models displays very close values with each other, showing a bias of underestimation with the CFD results.

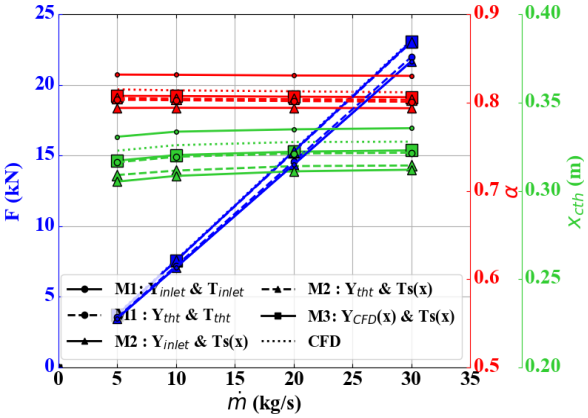

Figure 8: Net Thrust comparison between quasi-1D models and CFD, correlated with the thermal throat position when increasing the mass flow rate.

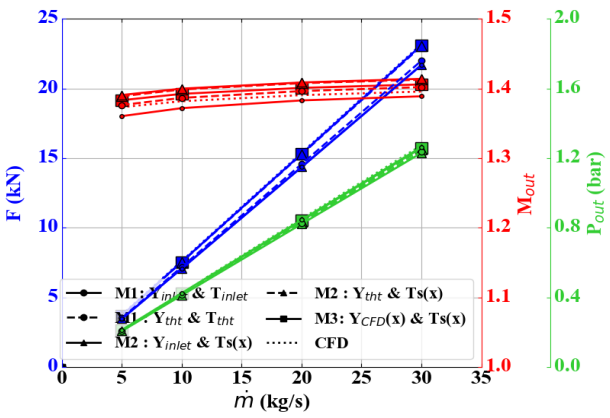

Figure 9: Outlet pressure and Mach number variations when increasing the inlet mass flow rate.

The Outlet Mach number shows very few variations when the mass flow rate increases due to the insensitiveness, in practice, of the thermal throat position. The Mach number profiles are strongly dependent on the heat addition gradient and the geometry. In the present case, the heat addition gradient is practically invariant with the mass flow rate due to the combustion model considering characteristic parameters of turbulence. Furthermore, the net thrust and the outlet pressure show a linear dependence on the mass flow rate, coherent with the definition of thrust and the conditions of the choked flow at the thermal throat.

As the equivalence ratio ($\phi = 1$) is the same for all the displayed computations in Fig. 12, the critical temperature remains unchanged with an increasing mass flow rate.

Copyright © 2024 by author(s)

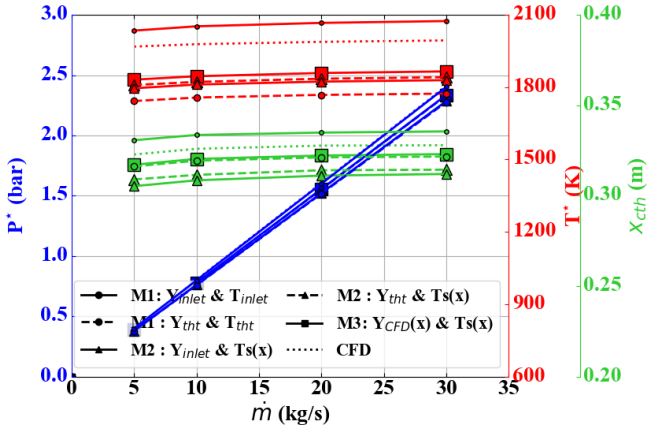

Figure 10 Variations of the critical conditions when increasing the inlet mass flow rate

Hence, the thermal throat position does not need to change. However, the change in mass flow rate implies a linear increase in the critical pressure. Thus, when increasing the mass flow rate, the pressure of the chamber increases but the Mach number field remains practically unchanged, depending mainly on the heat release gradient and the geometry of the divergent duct.

When considering the temperature dependence of the thermos-physical properties, model M3 underestimates the thermal throat position by about 1.7 %, whereas the M1 model with inlet species composition overestimates this value by about 2.3 %. The same trends are obtained with the critical temperature, highlighting the direct link with the thermal throat position via the cross-section area.

5.3. Effects of friction:

The friction on the wall is one of the main features of a viscous flow forming a boundary layer. For turbulent compressible flow found in a divergent duct with thermally choked flow, the friction drag is added in the equation of Zierep [2] at the thermal throat position. Hence, the friction drag has an impact on the thermal throat position, particularly on performances. Fig. 11 shows a comparison between the cases considering or not the friction in the equation of Shapiro [1].

With the friction drag, the thermal throat moves downstream about 2 % for both M1 and M2 models. Nevertheless, as stated without the friction effects, model M1, considering constant adiabatic coefficient displays a better agreement with the thermal throat position obtained by CFD simulations, except for the rich mixture. However, this approach must be used carefully due to the risk of compensating errors. With the friction drag term, the model M1 underestimates about 2 % of differences with the CFD simulations results for the thermal throat whereas the model M2 displays an averaged underestimation of 4 %. However, for the net thrust and the α coefficient, models M1 and M2 display very close differences compared with CFD results. Furthermore, the consideration of the friction term leads to reducing the differences of α coefficient, describing the thrust contribution of the subsonic part, from 4-5 % to 1-1.8 %. The same trend is also observed when increasing the mass flow rate (Fig. 12). Hence, the friction term contributes significantly to the accuracy of the quasi-one-dimensional models whatever the assumptions made on thermos-physical properties. Nevertheless, even though the consideration of friction improves results, the thermal throat and performance quantities remain underestimated. The addition of species distribution variation terms would improve the model as observed in the previous section.

Copyright © 2024 by author(s)

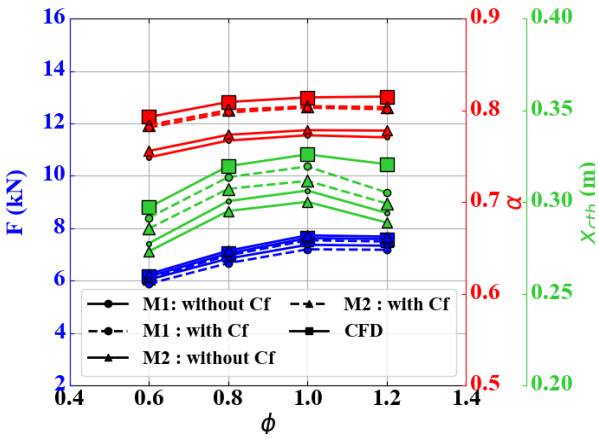

Figure 11: Effects of friction on thermal throat position and net thrust when increasing equivalence ratio.

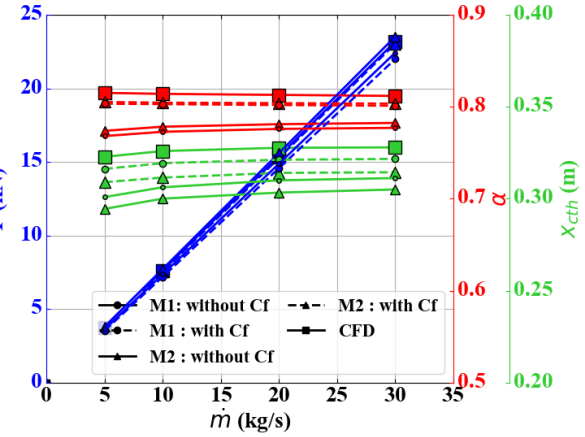

Figure 12: Effects of friction on thermal throat position and net thrust when increasing inlet mass flow rate.

6. Conclusion

A quasi-one-dimensional model for TCNF is developed to predict the potential performances of a dual-mode scramjet engine and to distinguish the associated contribution of considered physical phenomena involved in a TCNF. Three models based on the equations derived by Shapiro [1] are compared. The effect of friction is also considered to assess the impact on the parameters defining the TCNF. CFD simulations are carried out to validate the quasi-one-dimensional models.

The Mach number profiles show that a change in the thermal throat position shifts the Mach number profile, showing very similar trends between quasi-one-dimensional models. Furthermore, the Mach number variations are practically insensitive to the mass flow rate because of the invariance of the heat addition gradient in CFD simulations, probably caused by the turbulent combustion model. Future studies with kinetic mechanisms will be carried out to confirm the presented observations. The equivalence ratio plays an essential role in TCNF for predicting performance. When increasing the equivalence ratio for a lean mixture, the critical temperature at the thermal throat increases. Assuming a constant mass flow rate, the choked flow conditions imply the increase of the cross-section area and the critical pressure. In a divergent nozzle, these conditions lead to moving the thermal throat position downstream. The thrust increases because of the increase of the outlet temperature and pressure, even though the outlet Mach number decreases due to the closeness of the thermal throat to the exit. The model M3 displays the best prediction in net thrust and thermal throat position due to the good agreement of outlet conditions with the CFD results. However, the critical conditions are not following the same trend. Furthermore, the dependence on species is strong to obtain those results. The model M3 requires complementary analysis with other test cases to assess the robustness of the approach. Nevertheless, the model M1 with inlet species composition displays critical conditions surprisingly better reproduced. The differences in Mach number and thermodynamic conditions are more important close to the inlet due to the complex flow evolving downstream of the flame-holders. Besides, the friction coefficient provides a significant contribution to the thermal throat location.

However, complementary analysis is required to extend the methodology to other geometries (angle of aperture) and to be able to integrate a fully multi-species method with finite rate chemistry for prediction performances of the TCNF. In the future, 3D simulations for the reference case will be considered to reduce the impact of injection and flame-holder systems on the flow and to obtain more physical data.

References

1. Torrez, S., Driscoll, J., Bolender, M., Oppenheimer, M., & Doman, D. (2008). Effects of improved propulsion modelling on the flight dynamics of hypersonic vehicles. In *AIAA Atmospheric Flight Mechanics Conference and Exhibit* (p. 6386).

Copyright © 2024 by author(s)

2. Torrez, S. M., Driscoll, J., Dalle, D., and Daniel Micka. "Scramjet Engine Model MASIV: Role of Mixing, Chemistry and Wave Interaction," AIAA 2009-4939. *45th AIAA/ASME/SAE/ASEE Joint Propulsion Conference & Exhibit*. August 2009.
3. Torrez, S. M., Driscoll, J., Dalle, D., Michael Bolender and David Doman. "Hypersonic Vehicle Thrust Sensitivity to Angle of Attack and Mach Number," AIAA 2009-6152. *AIAA Atmospheric Flight Mechanics Conference*. August 2009.
4. Torrez, S. M., Driscoll, J., Dalle, D., and Fotia, M. "Preliminary Design Methodology for Hypersonic Engine Flowpaths," AIAA 2009-7289. *16th AIAA/DLR/DGLR International Space Planes and Hypersonic Systems and Technologies Conference*. October 2009.
5. O'Brien, T. F., Starkey, R. P., and Lewis, Mark J., Quasi-One-Dimensional High-Speed Engine Model with Finite-Rate Chemistry, Journal of Propulsion and Power 2001 17:6, 1366-1374.
6. Shapiro, A., The Dynamics and Thermodynamics of Compressible Fluid Flow, Vol. 1, Ronald Press, New York, pp. 226-227
7. Birzer, C. H., & Doolan, C. J. (2009). Quasi-one-dimensional model of hydrogen-fueled scramjet combustors. *Journal of propulsion and power*, *25*(6), 1220-1225.
8. Torrez, S. M., Driscoll, J. F., Ihme, M., & Fotia, M. L. (2011). Reduced-order modeling of turbulent reacting flows with application to ramjets and scramjets. *Journal of propulsion and power*, *27*(2), 371-382.
9. Ispir, A.C., and Saracoglu, B.H. "Development of a 1D dual mode scramjet model for a hypersonic civil aircraft," AIAA 2019-3842. *AIAA Propulsion and Energy 2019 Forum*. August 2019.
10. Torrez, S. M., Dalle, D. J., & Driscoll, J. F. (2013). New method for computing performance of choked reacting flows and ram-to-scram transition. *Journal of Propulsion and Power*, *29*(2), 433-445.
11. Zhang, D., Feng, Y., Zhang, S., Qin, J., Cheng, K., Bao, W., & Yu, D. (2016). Quasi-one-dimensional model of scramjet combustor coupled with regenerative cooling. *Journal of Propulsion and Power*, *32*(3), 687-697.
12. Cakir, B. O., Ispir, A. C., & Saracoglu, B. H. (2022). Reduced order design and investigation of intakes for high speed propulsion systems. *Acta Astronautica*, *199*, 259-276.
13. Connolly, B. J., Krouse, C. R., & Musgrove, G. O. (2021). Implementing a dual-mode scramjet combustor model in NPSS. In *AIAA Propulsion and Energy 2021 Forum* (p. 3538).
14. Smart, M. (2007). Scramjets. *The Aeronautical Journal*, *111*(1124), 605-619
15. Heiser, W. H., & Pratt, D. T. (1994). *Hypersonic airbreathing propulsion*. Aiaa.
16. Li, J., Jin, R., Jiao, G., & Song, W. (2018). Analysis on mode transition in a dual-mode scramjet combustor. *Combustion Science and Technology*, *190*(1), 82-96.
17. Seleznev, R. K. (2017, February). Comparison of two-dimensional and quasi-one-dimensional scramjet models by the example of VAG experiment. In *Journal of Physics: Conference Series* (Vol. 815, No. 1, p. 012007). IOP Publishing.
18. Tian, L., Chen, L., Chen, Q., Li, F., & Chang, X. (2014). Quasi-one-dimensional multimodes analysis for dual-mode scramjet. *Journal of Propulsion and Power*, *30*(6), 1559-1567.
19. Dechant, L. J., & Tattar, M. J. (1994). *Analytical skin friction and heat transfer formula for compressible internal flows* (No. NASA-CR-191185).
20. Zierep, J., & Kuchemann, D. (1974, May). Theory of flows in compressible media with heat addition. AGARD.
21. Olivon, F., Durand J.E., Genot, A., and Piot, E., Unsteady Forced Motion of the Thermal Throat in a Low-Mach Dual-Mode Ramjet Nozzle, *10th European Conference for Aerospace Sciences*, Paper 558, Lausanne, Switzerland.

Copyright © 2024 by author(s)